SCEC-NASA Collaborative Proposal: Database Development for the Trona Pinnacles Fragile Geologic Features

Report for SCEC Award #20119

Investigators and contributors: Christine A. Goulet[1], Xiaofeng Meng[1], Andrea Donnellan[2], Greg Lyzenga[2], Devin McPhillips[3], Savannah Devine[4]

INTRODUCTION

Damage sustained by Fragile Geologic Features (FGFs) can help constrain the level of ground motions in the absence of instruments (Brune 1996; Anderson et al. 2011 and 2014; Grant et al. 2015). The determination of the upper limits of ground motions is a key knowledge gap for the design of critical infrastructure such as nuclear repositories, power plants or even dams. FGFs damaged by strong earthquake shaking can provide constraints on the level of such extreme ground motions. The observation of damaged versus undamaged FGFs following earthquakes is critical in calibrating and validating FGF ground motion assessment methodologies developed from lab experiments and numerical modeling (e.g. Anooshehpoor et al. 2004; 2013).

The close proximity of the Trona Pinnacles National Monument and 2019 Ridgecrest earthquake sequence provides an unique opportunity to investigate the damage of FGFs by strong ground shaking, which we observed during reconnaissance activities. Because of the Covid-19 pandemic, we could not conduct the proposed comprehensive field survey of the Trona Pinnacles. However, we still made great progress in three areas, even though some of the tasks required more work when converted to desktop activities. First, we have a prototype database of spires at Trona Pinnacles that includes all the images and data collected from post-Ridgecrest field surveys and from additional internet search. Second, tensile strength of selected spires were measured and analyzed. Third, several sUAS surveys were conducted. Point clouds were generated from the surveys and used to identify damage caused by a M5.6 aftershock.

PROGRESS REPORT

In this section, we provide progress on the tasks outlined in our proposal, which are listed in the subsections below. Tasks 1, 2 fed directly into Task 6 and the experience form gathering information on spires and photographs directly fed into the database structure development. Data from Task 3 is an important part of the database development, which will help constrain the upper bound of ground motions. Without in-person visit to Trona Pinnacles, the point clouds obtained from Tasks 4 and 5 served as a crucial complementary data to GoogleEarth to identify spires from internet photographs in task 1.

1. Field identification of structures and photographic documentation

Although field visits were not possible due to the Covid pandemic, we have been able to identify and develop a nomenclature for the spires using photographs taken during the Ridgecrest post-event reconnaissance by Meng and Goulet. This desktop approach required more work to organize the photographs and their content, since getting a field perspective to get familiar with individual spires was not possible.

The first step was to get familiar with the area and carefully review the pictures, which were imported in GoogleEarth based on their geotag locations. In GoogleEarth, we identified each pinnacle or feature (pinnacles consist of individual spires or groups of spires) that was documented, and assigned each pinnacle a unique identification (ID) number. The pinnacles were further organized into clusters based on their general location and accessibility. Using this GoogleEarth file in conjunction with point clouds was critical in identifying each feature in all of the field photographs. The list of pinnacles in each photograph was compiled using a combination of matlab codes and spreadsheets. A GoogleEarth file was created for sharing that includes the pinnacles and their unique ID.

2. Desktop collection of dated pre-event pictures

We performed a thorough internet search for pre-Ridgecrest images of the Trona Pinnacles, exploring travel blogs, government websites, Instagram accounts, and other relevant social media platforms. If the contact information of the photographer was available, we reached out in order to gain permission to include the images in the database and to gain information about the image capture date. Only images with clear information on the capture date were retained. Once permission was granted, we identified the pinnacles defined in Task 1, and added the photograph information to our database.

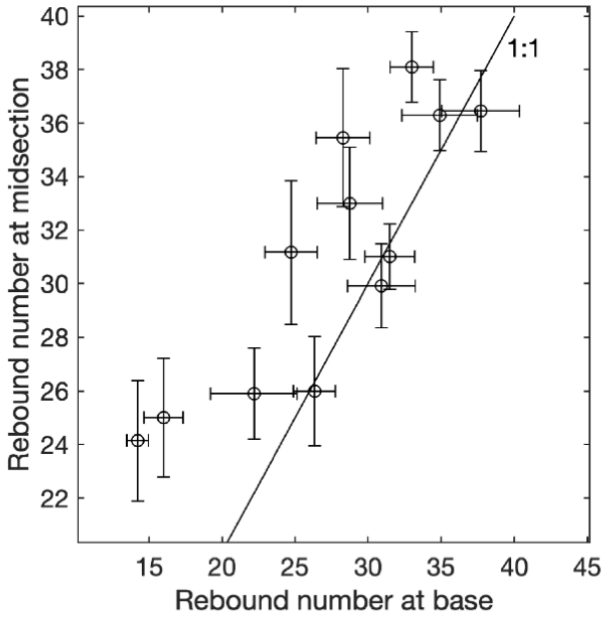

Figure 1. Rebound number comparison between measured at midsection and base.

3. Field measurement of tensile strength of selected spires

In order to characterize the fragility of the pinnacles, it is essential to understand their material strength. To date, we have made in situ strength measurements at 10 pinnacles using an L-type Schmidt Rebound Hammer. We measured the rebound number more than 200 times, on different parts of each pinnacle, paying careful attention to the tufa facies. We scaled the rebound number through unconfined compressive strength to estimate tensile strength (Wang et al., 2016; Perras and Dieterichs, 2014). On average, the scaled tensile strength of the phytoherm boundstone and framestone facies at Trona is 1.4 MPa, which is consistent with laboratory-derived measurements from Antalya tufa in Turkey (Sopaci et al., 2015). Perhaps the most interesting result is from a comparison of the rebound numbers measured at different positions on the pinnacles (Figure 1). We find that the rebound numbers measured at the bases of the

pinnacles are consistently lower than those measured higher up. This result is consistent with material weakening at the bases due to fractures created during earthquake shaking.

4. Field sUAS surveys of selected spires and rocks

We conducted a synoptic survey of the majority of the Trona Pinnacles. We flew a Parrot Anafi small uninhabited aerial vehicle (sUAVS) or drone around the pinnacles and fallen rocks of interest at different altitudes and cover double grids over large sections of the pinnacles. We had flown grids over the western cluster of pinnacles on 2019-09-27. The grid covered 0.415 km^2 (or about 600 x 700 m). On 2020-06-03, a M5.5 aftershock occurred at latitude 35.615°N, longitude 117.428°W and 8.4 km depth, 5 km west of the pinnacles we had flown in September 2019. We then returned to fly other grids on 2020-06-10, 2020-06-29, and 2020-08-07. As a likely result of the aftershock, we noted during our 2020-06-10 survey that one of the spires was damaged, leaving it disintegrated into a boulder, a rock, and a debris field at the top of the pinnacle and two boulders at its base. During all our visits, we surveyed several pinnacles, and performed subsequent point cloud comparisons (Task 5) in an attempt to find other cases of damage from known aftershocks, and to evaluate the evolution of the pinnacles integrity.

5. Cloud point evaluation of volumes from sUAS surveys

We processed the data with the commercial software package Pix4D that uses stereophotogrammetric or structure from motion (SfM) techniques to compute point clouds and digital surface models of the features of interest. Average ground sample distance (GSD) is about 3 cm for the large-scale surveys and about 1 cm for the surveys targeting a single feature or pinnacle. We did not use ground control points (GCPs), however analysis of other data we have collected indicates the overall geometry is accurate to a few cm and the absolute positions of the surveys is better than 0.5 m. We used Pix4D to calculate volumes of intact spires as well as fallen debris. We used Cloud Compare to compare point clouds from before and after the aftershock. We finely aligned the point clouds and then computed 3D cloud to cloud comparisons. All of the point clouds differenced for before and after the 2020-06-03 aftershock show the presence of only three small changed spots in the entire area. These changes mark the new presence of boulders. The top of Pinnacle 6 (P006) also shows a change between point clouds. Visual comparison of the before point cloud and individual aerial images shows a large spire at the top of P006 along its ridge that is not present in the post- aftershock point clouds or images.

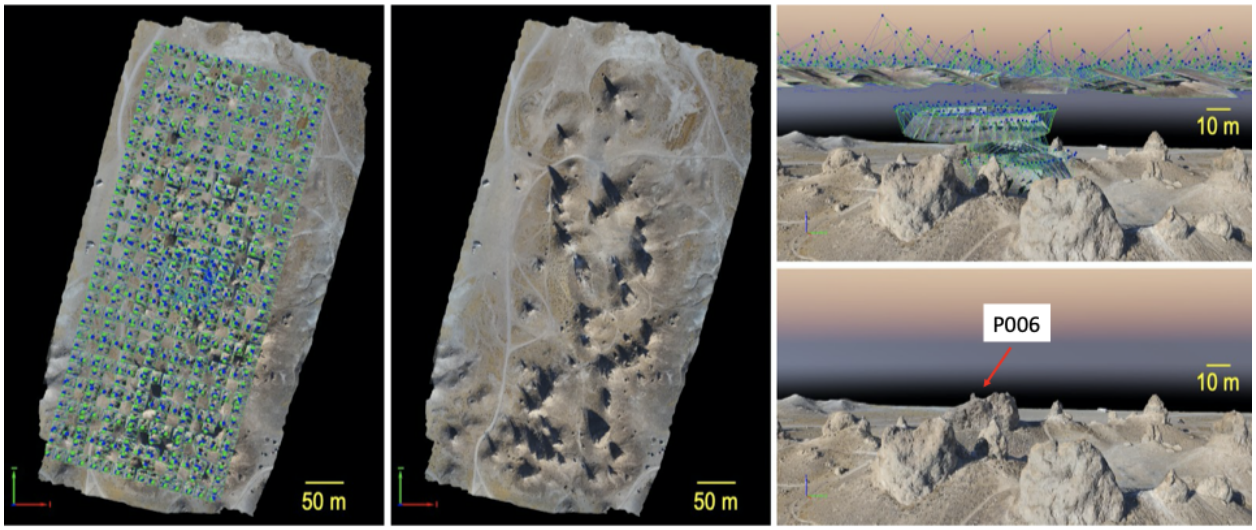

Figure 2. Snapshot of point clouds and digital surface models from the small Unmanned Aircraft System surveys. Left: Flight grid (blue and green dots) overlayed on the digital surface model of Trona Pinnacles. Middle: The digital surface model of Trona Pinnacles. Top right: Circular flight paths around selected spires. Bottom right: Digital surface model of selected spires.

6. Development of html/xml database

Based on the data collected, we created a prototype database that consists of three linked tables: spires, images and photographers. The spires table contains one entry for each feature, including its unique ID, the list of images that it appeared in as well as relevant information collected from the images and field measurements (e.g., location coordinates, tensile strength). The images table lists all the images collected from internet (mostly pre-event) and field survey photographs (both pre- and post-event), their basic information (e.g., date taken, photographer, location coordinates) and the IDs of spires appearing in the images, which are linked to the spires table. The photographers table consists of each photographer's name, contact information and the list of images they took, which is linked to the images table. The description of each field for the three tables are summarized in Tables 1-3. The tables are generated by Matlab using the GoogleEarth file and aggregating the collected data on spires, images and photographers. Google tables was found to be the best option for the implementation of the prototype database, because it is open source and allows for collaborative access. Moreover, it is easier to use and interact with than conventional database frameworks.

Table 1. Spire table content

Field name	Short name	Description	Variable type
*Unique ID**	ID	Unique ID for each feature	Integer
FGF Name	Name	The ID given to each spire from .KML file	String
Photographs	Photo	Photographs that include each spire	Image
General Notes	Notes	Any information not included in other fields	String
Location	Location	The lat/lon coordinates of each spire	Number
Location Descriptor	Descriptor	Something to describe the general location of	String

		each spire	
Geology	Geology	Notes of the general geologic properties of each feature	String
Cluster	Cluster	Cluster ID that eachs spire belongs to	String
Strength Measurements	Strength	Strength measurements of each feature	Number
alpha 1 and 2	alpha 1 and 2	Angle between vertical direction and the direction from the mass center to rocking points	Number
r 1 and 2	r 1 and 2	Distance between the mass center and rocking points	Number
Aliases	Aliases	Aliases for each feature	String

* Link to image table

Table 2. Photographer table content

Field name	Short name	Description	Variable type
*Photographer ID**	ID	Unique numerical ID given to each photographer	Integer
Name	Name	Name of photographer	String
Email address	Email	Email	String
Photos Taken	Photos	The list of photos taken by each photographer	List
Website	Website	Link to photographer's website	String
Social media handle	Social media	Social media handle of each photographer	String

*Link to image table

Table 3. Image table content

Field name	Short name	Description	Variable type
Photo ID	ID	Unique numerical ID	Integer
File name	Name	Full path of each image	String
*Spires List**	Spires	IDs of spires that are included in each image	List
*Photographer^*	Photographer	ID of photographer	Integer
Date taken	Date	Date photo was taken	Date
Notes	Notes	Any other relevant information not included in other fields	String

*Link to spire table
^Link to photographer table

REFERENCES

Anderson, J. G., Biasi, G. P., & Brune, J. N. (2014). Precarious rocks: providing upper limits on past ground shaking from earthquakes. In Wyss, M. (Ed.), Earthq. Haz. Risk Disast., Elsevier, Inc., (pp. 377-403).

Anderson, J.G., Brune, J.N., Biasi, G.P., Anooshehpoor, A., and Purvance, P. (2011). Workshop Report: Applications of Precarious Rocks and Related Fragile Geological Features to U.S. National Hazard Maps, Seism. Res. Lett., v. 82, no. 3, p. 431-441.

Anooshehpoor, A., Brune, J. N., and Zeng, Y. (2004). Methodology for obtaining constraints on ground motion from precariously balanced rocks. Bull. Seism. Soc. Am., 94(1), 285–303.

Anooshelpoor et al., 2013, Constraints on Ground Accelerations Inferred from Unfractured Hoodoos near the Garlock Fault, California. BSSA, 103(1), 99-106.

Brune, J. N. (1996). Precariously balanced rocks and ground-motion maps for southern California. Bull. Seism. Soc. Am., 86(1), 43–54.

Grant Ludwig, L., Brune, J. N., Anooshehpoor, A., Purvance, M. D., Brune, R. J., and Lozos, J. C. (2015) Reconciling precariously balanced rocks (PBRs) with large earthquakes on the San Andreas fault system, Seism. Res. Lett., 85, 1345-1353.

Perras, M.A., and M.S. Diederichs (2014). A Review of the tensile strength of rock: Concepts and testing, Geotech. Geol. Eng. 32, 525-546

Sopaci, E, and H. Akgun (2015). Geotechnical assessment and engineering classification of the Antalya tufa rock, southern Turkey, Engineering Geology, 197, 211-224.

Wang, H., H. Lin, and P. Cao (2016). Correlation of UCS rating with Schmidt Hammer surface hardness for rock mass classification, Rock Mech. Rock Eng. DOI 10.1007/s00603-016-1044-7